Journal of Applied Physics ARTICLE scitation.org/journal/jap

Influence of oxygen on trap-limited diffusion of hydrogen in proton-irradiated *n*-type silicon for power devices

Cite as: J. Appl. Phys. **129**, 025701 (2021); doi: 10.1063/5.0035260
Submitted: 27 October 2020 · Accepted: 16 December 2020 ·
Published Online: 8 January 2021

Akira Kiyoi,[1,2,a)] Naoyuki Kawabata,[1] Katsumi Nakamura,[3] and Yasufumi Fujiwara[2]

AFFILIATIONS

[1]Advanced Technology R&D Center, Mitsubishi Electric Corporation, 8-1-1 Tukaguchi-Honmachi, Amagasaki, Hyogo 661-8661, Japan
[2]Division of Materials and Manufacturing Science, Graduate School of Engineering, Osaka University, 2-1 Yamadaoka, Suita, Osaka 565-0871, Japan
[3]Power Device Works, Mitsubishi Electric Corporation, 1-1-1 Imajuku-Higashi, Nishi-ku, Fukuoka, Fukuoka 819-0192, Japan

[a)]**Author to whom correspondence should be addressed:** Kiyoi.Akira@ay.MitsubishiElectric.co.jp

ABSTRACT

The growing demand for power devices has led to the use of magnetic field-applied Czochralski (m:Cz) wafers owing to the limited production capacity and available diameters of the traditionally used floating zone (FZ) wafers. Consequently, the influence of oxygen impurities in the wafers on the electrical properties of devices, regardless of the growth method, needs to be investigated to achieve a stable fabrication process for power devices. Using the proton irradiation doping process and spreading resistance profiling technique, we evaluated the effective diffusion coefficient (D_{eff}) related to trap-limited diffusion of hydrogen and the effects of impurities on diffusivity. We irradiated *n*-type silicon wafers, which have different carbon, oxygen, and phosphorus concentrations, with 2 MeV protons and annealed them at 300–400 °C. By analyzing the width of the *n*-type region, where hydrogen-related shallow donors (HDs) are induced, we estimated D_{eff} to be five to six orders of magnitude lower than the intrinsic diffusion coefficient, indicating that hydrogen motion is highly trap-limited. D_{eff} was significantly dependent on the oxygen concentration, and the activation energy of hydrogen diffusion varied from 0.57 ± 0.15 eV (pure epitaxial wafer) to 2.19 ± 0.15 eV (m:Cz wafer). This trend suggests that oxygen-related defects preferentially trap the mobile hydrogen released from thermally dissociated HDs. This study also reveals that the diffusion coefficients of different materials when annealed at 400 °C are comparable. This information is essential to realize the cost-effective production of power devices because we can treat m:Cz and FZ wafers equivalently during the doping process.

I. INTRODUCTION

Floating zone (FZ) grown silicon wafers, which are impurity-lean and defect-free, have been conventionally used as the starting material in the production of power semiconductor devices such as insulated gate bipolar transistors (IGBTs).[1] However, the recent growth in demand for power devices cannot be met by FZ wafers alone owing to their limited production capacity and the technological difficulty in fabricating larger wafer diameters using this growth method. Recently, another type of silicon wafer grown by the magnetic-applied Czochralski (m:Cz) method has become a standard starting material for power devices, in addition to FZ wafers.[2]

There is a major difference between m:Cz wafers and conventional FZ wafers regarding the production of power devices. The oxygen concentration of m:Cz wafers is commonly more than two orders of magnitude higher than that of the conventional FZ wafers. In addition, carbon concentration is often adjusted to control oxygen precipitation nucleated at carbon sites during the growth of m:Cz wafers.[3]

The demand for high-performance IGBTs requires an understanding of the influence of the relevant impurities in the silicon material. The presence of carbon and oxygen affects the electrical properties of IGBTs when the devices are irradiated with electrons, protons, and helium ions for conventional life-tailoring or

production of broad *n*-type field-stop layers.[2,4,5] Carbon was discussed as a source of instability in the production of IGBTs based on m:Cz wafers.[4] In Ref. 4, the trade-off between switching losses and forward voltage drop was correlated with the annealing characteristics of the carbon-related defects observed from photoluminescence studies. The high oxygen concentration in m:Cz was considered to be a source for enhancing the formation of proton irradiation-induced donors in the field-stop layers.[2] Such donors have been called hydrogen-related donors (HDs) and have been phenomenologically speculated to be defect complexes decorated with hydrogen. These complexes have been reported to have a shallow-donor level with an ionization energy of 34–53 meV.[6–13] However, the formation and dissociation mechanisms of HDs have not yet been identified.

Laven *et al.* studied the formation kinetics of HDs in proton-irradiated *n*-type FZ silicon and discussed the relevant diffusion coefficient of hydrogen by analyzing the spreading resistance (SR) profiles.[12,13] They reported that hydrogen exhibited trap-limited diffusion, where effective diffusion of hydrogen had a relatively large activation energy of 1.2 eV in the proton-penetrated layer.[12,13] However, they mainly focused on FZ wafers and did not fully discuss the effects of impurities on the diffusivity of hydrogen. In the implementation of proton irradiation doping to produce the field-stop layer in IGBTs, the effective diffusion coefficient of hydrogen limits the width of the layer produced. Therefore, investigating the peculiarities of hydrogen diffusivity in m:Cz silicon and understanding the interaction between impurities and hydrogen are important for developing next-generation IGBTs and advancing hydrogen-related silicon technology.

In the present study, we investigated the effective diffusion coefficient of hydrogen and its interaction with impurities, aiming to effectively apply proton irradiation doping to power devices. Four types of silicon wafers comprising m:Cz, FZ, and epi silicon were irradiated with 2 MeV protons, subsequently annealed at 300–400 °C for 1–25 h and analyzed by SR profiling measurements. Owing to the reaction between hydrogen and irradiation-induced defects, an additional *n*-type doping region was created in the deep wafer region depending on the annealing temperature and time. By analyzing the expansion of the doping region, effective diffusion coefficient and activation energy for hydrogen diffusion were deduced. In addition, the influence of carbon and oxygen concentrations in silicon wafers on the deduced diffusion coefficient of hydrogen was considered.

II. EXPERIMENT

We used four types of phosphorous-doped *n*-type silicon wafers with different concentrations of phosphorus, carbon, and oxygen. The wafers were (100)-oriented and had a thickness of approximately 725 μm. The carbon and oxygen concentrations were measured by secondary ion mass spectrometry (CAMECA IMS-7f) using a Cs^+ primary ion beam with an energy of 14.5 eV. The phosphorus concentration was estimated from the carrier concentration of the bulk, which was measured by the SR profiling method. The phosphorus, carbon, and oxygen concentrations of each wafer are summarized in Table I.

TABLE I. List of impurity concentrations in wafers.

Wafers	P concentration (cm^{-3})	C concentration (cm^{-3})	O concentration (cm^{-3})
FZ (77)	5.5×10^{13}	6.3×10^{14}	$<5.0 \times 10^{15}$
FZ (715)	7.5×10^{12}	1.8×10^{15}	$<5.0 \times 10^{15}$
m:Cz (77)	5.5×10^{13}	1.1×10^{15}	1.8×10^{17}
epi (60)	5.1×10^{13}	$<5.0 \times 10^{14}$	$<5.0 \times 10^{15}$

Wafers were irradiated by 2 MeV protons at a dose of 3×10^{14} cm^{-2} using a cyclotron particle accelerator. The projection range of the irradiation was estimated to be 44 μm deep from the incident surface. To avoid unintentional annealing caused by high-dose irradiation, irradiation was performed intermittently to maintain the temperature of the wafers at less than 150 °C. After irradiation, wafers were cut into samples of suitable size and annealed at a temperature of 300–400 °C in an oven under an air atmosphere. The actual temperature of samples was monitored by a thermocouple placed close to the sample. The annealing time was varied from 1 to 25 h. After annealing, samples were removed from the oven and immediately immersed in water in order to bring them to room temperature (~25 °C).

Samples were measured and analyzed by two-point SR profiling at room temperature with a spreading resistance profiler (SSM-2000 from Solid State Measurements, Inc.). Prior to the measurements, samples were beveled at an angle of approximately 2.5° to achieve an adequate depth resolution of 0.25 μm. The measured SR profiles were transformed into the equivalent carrier concentration profiles via calibration with a standard silicon wafer, assuming that all regions exhibited *n*-type conductivity.

III. RESULTS AND DISCUSSION

A. Carrier concentration profiles

We first discuss the typical carrier concentration profile produced by a high dose of proton irradiation. Figure 1 shows the carrier concentration profile of an FZ (77) sample irradiated

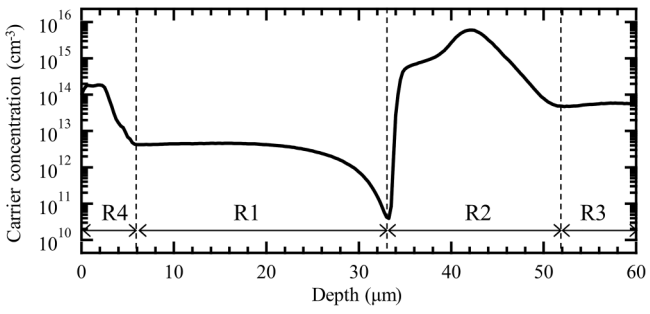

FIG. 1. Typical carrier concentration profile formed by high-dose proton irradiation and subsequent annealing at a moderate temperature. The figure shows the carrier concentration profile of an FZ (77) sample annealed at 325 °C for 9 h. R1–R4 indicate characteristic regions, as described in the text.

with 2 MeV protons and subsequently annealed at 325 °C for 9 h. For an irradiation energy of 2 MeV, the penetration depth of protons into silicon was estimated to be 44 μm by the transport of ions in matter calculation.[14] Owing to the high concentration of radiation-induced defects distributed across the penetrated layer, hydrogen is coupled with the defects, creating a unique carrier concentration profile on its out-diffusion pathway. The characteristic regions are depicted as R1–R4 in Fig. 1. In the penetrated region (R1 in Fig. 1), the concentration of acceptor-type defects induced by the irradiation[12,13] is higher than that of the donor species. In the case of highly resistive *n*-type wafers, such as those used in the present study, acceptor-type defects easily induced conduction-type inversion from *n*-type to *p*-type. In the region where the protons penetrated and stopped (R2 in Fig. 1), sufficient hydrogen and radiation-induced defects coexisted; thus, HDs were formed adequately to prevent conduction-type inversion (HDs have been considered to be defect-hydrogen complexes, which have donor states. See Refs. 6–13 for details.). Consequently, a *p-n* junction was formed between R1 and R2, which appears as a dip at a depth of 33 μm in Fig. 1. The region beyond the penetration depth of the proton (R3 in Fig. 1) denotes the unaffected substrate region. In this region, the carrier concentration depends only on the dopant (P) concentration of the wafers. Near the surface (R4 in Fig. 1), other types of donors were formed. The origin of these donors has not been ascertained; however, they seem to be oxygen-related thermal donors (TDs) enhanced by the existence of radiation-induced vacancy-type defects and implanted hydrogen.[15–17]

Figure 2 shows a comparison of the carrier concentration profiles of different silicon wafers annealed at 350 °C for 1, 4, 9, and 25 h. We define the diffusion-front depth of hydrogen in R1, *d*, at which the carrier concentration becomes equal to the uniform bulk carrier concentration in R3. In Fig. 2, *d* for each profile is indicated by the dotted arrows. For example, the position of *d* for the FZ (77) samples [Fig. 2(a)] shifts from 34.5 to 27 μm as the annealing time increases from 1 to 25 h. This shift is probably induced by the out-diffusion of implanted hydrogen and its reaction with irradiation-induced defects in the out-diffusion pathway. The carrier concentration profiles of the FZ (715) samples [Fig. 2(b)] and epi (60) samples [Fig. 2(c)] also have features similar to those observed in the FZ (77) samples. However, the position shift of *d* is larger for the epi (60) samples than that observed in the FZ samples under equivalent annealing conditions. For the m:Cz (77) samples [Fig. 2(d)], the carrier concentration profiles show additional *n*-type regions in the vicinity of the penetration depth, and the expansion of this region occurs toward the surface as well as the FZ and epi samples. However, the position shift of *d* for the m:Cz (77) samples is much smaller than that observed for the FZ samples under equivalent annealing conditions. Therefore, it is determined that the effective diffusion length of hydrogen strongly depends on the silicon material at the given annealing temperature and time.

In addition, the carrier concentration profiles of m:Cz (77) samples exhibit no *p-n* junctions, although the carrier concentration profiles of the FZ and epi samples have *p-n* junctions, accompanied by HD formation at all annealing times. Owing to the high oxygen concentration of 1.8×10^{17} cm^{-3} in m:Cz silicon, oxygen-related TDs were induced massively in the penetrated region and probably compensated for the radiation-induced acceptor-type defects.

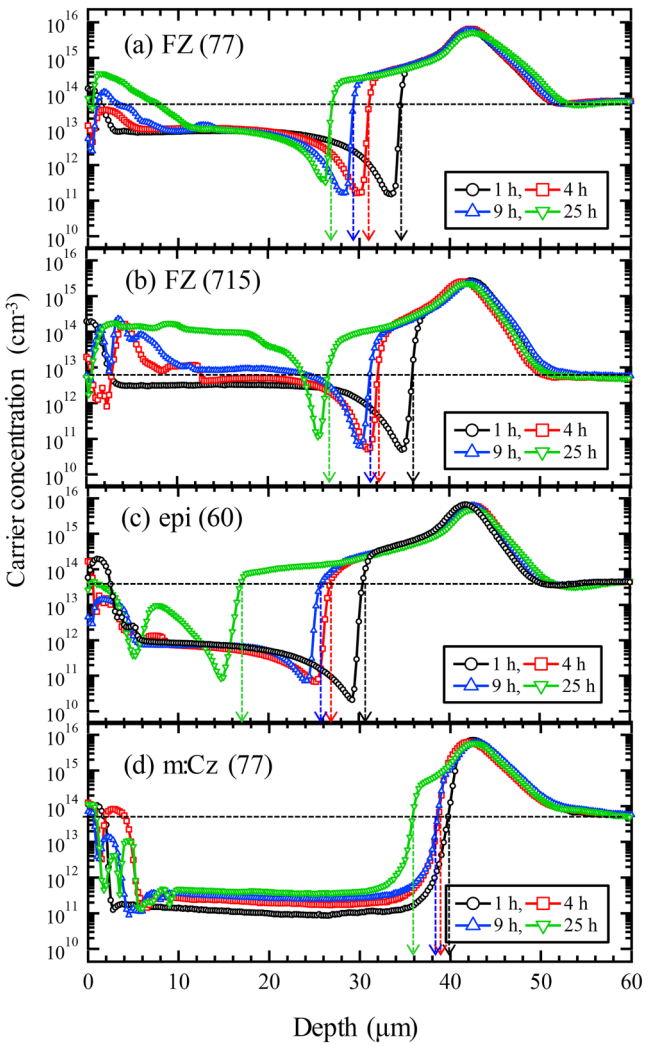

FIG. 2. Carrier concentration profiles of the (a) FZ (77), (b) FZ (715), (c) epi (60), and (d) m:Cz (77) samples after the implantation of 2 MeV protons with a dose of 3×10^{14} cm^{-2} and annealing at 350 °C for different periods. Carrier concentration profiles of samples annealed for 1, 4, 9, and 25 h are denoted by circles, squares, triangles, and inverted triangles, respectively. Dotted arrows indicate the diffusion-front depth of hydrogen, *d*, as defined in the text.

Figure 3 shows the carrier concentration profiles of FZ (77) and m:Cz (77) samples annealed at different temperatures (325, 350, 375, and 400 °C) for different periods of time (1, 4, 9, and 25 h). The HDs were induced in the deep wafer region in the range of 300–400 °C, and diffusion-like expansion of the additional *n*-type region is observed between R1 and R2 under all annealing conditions. Concurrently, a slight decay of HD concentration was observed in R2 at over 350 °C in all samples. The variations in the effective

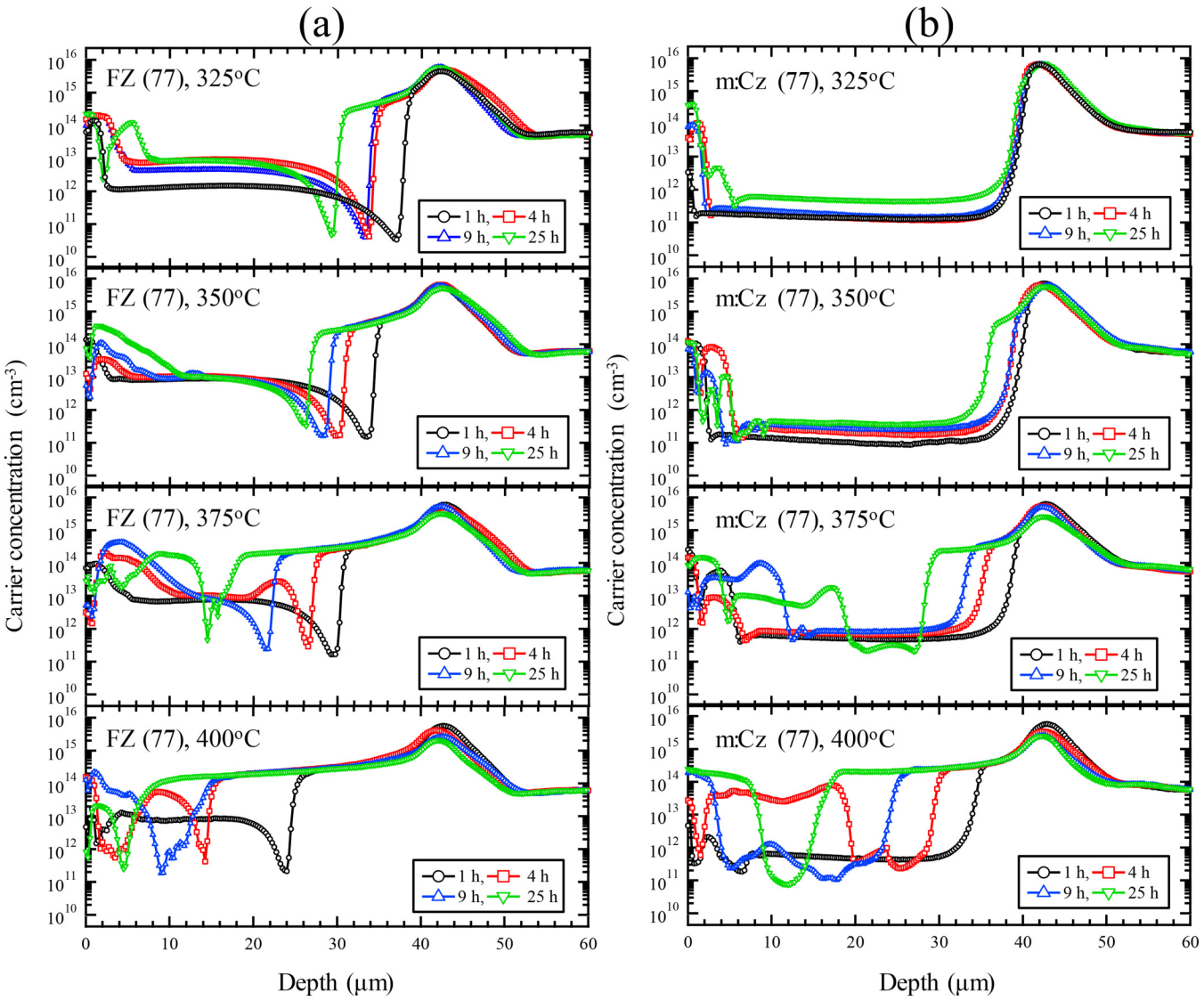

FIG. 3. Carrier concentration profiles of the (a) FZ (77) and (b) m:Cz (77) samples after the implantation of 2 MeV protons with a dose of 3×10^{14} cm^{-2} and subsequent annealing at 325, 350, 375, and 400 °C for different periods. Carrier concentration profiles of samples annealed for 1, 4, 9, and 25 h are denoted by circles, squares, triangles, and inverted triangles, respectively.

diffusion coefficient and activation energy of hydrogen diffusion with depth d are discussed in Sec. III B.

B. Diffusivity of hydrogen

The slowed-down diffusion of hydrogen is characterized by defect-mediated effective diffusivity. Even in this case, the diffusion of hydrogen can be described by Fick's second law of diffusion. The temperature dependence of D_{eff} follows the Arrhenius equation, which is expressed as

$$D_{\text{eff}} = D_0 \exp(-E_a/kT), \quad (1)$$

where D_0 is a pre-exponential factor, E_a is the activation energy of diffusion, k is the Boltzmann constant, and T is the annealing temperature.

Figure 4 shows d as a function of the square root of t. Using the simplified expression,[13] d is described as

$$d = d_0 - \sqrt{(4D_{\text{eff}}t)}, \quad (2)$$

where d_0 is the depth at which the implanted hydrogen starts to diffuse and t is the annealing time. d_0 should ideally correspond to the penetration depth, where implanted hydrogen is localized

immediately after irradiation. However, d_0 is distributed because the implanted hydrogen migrates owing to additional annealing during irradiation.

As indicated in Fig. 4, d decreases with the square root of t, as expected for a diffusion-limited process. By fitting the data linearly, we obtained the effective diffusion coefficient D_{eff} of hydrogen according to Eq. (2). Figure 5 shows D_{eff} as a function of reciprocal temperature together with the extrapolated line from the Van Wieringen and Warmoltz (VWW) relationship.[18] The experimentally obtained values of D_{eff} are five to six orders of magnitude lower than the values extrapolated from the VWW relationship, which is calculated as $D = 9.43 \times 10^{-3} \exp\ (-0.48\ \mathrm{eV}/kT)\ \mathrm{cm}^2/\mathrm{s}$. The VWW relationship was deduced from a high temperature (1090–1200 °C) permeation experiment; thus, it is interpreted as the intrinsic diffusion coefficient of isolated hydrogen in silicon crystals without any trapping effects. Therefore, it is reasonable that the extrapolation of the VWW relationship to a moderate temperature, at which the trapping effect has to be considered, demonstrates higher values than experimentally obtained effective diffusion coefficients.[18–37] Our results suggest that hydrogen diffusion in our samples is a trap-limited diffusion process. In the case of epi wafers, which are extremely pure, the trapping centers for hydrogen are mainly intrinsic point defects (i.e., vacancy or self-interstitial agglomerates induced by proton irradiation). However, in the case of FZ and m:Cz wafers, the effects of additional traps related to oxygen and carbon on D_{eff} should be considered.

It is also clearly observed in Fig. 5 that D_{eff} decreases as the oxygen concentration increases from less than 5×10^{15} to $1.8 \times 10^{17}\ \mathrm{cm}^{-3}$ when comparing the epi and FZ samples with the m:Cz samples. The dependence of D_{eff} on the oxygen concentration becomes less prominent with increasing annealing temperature. These results indicate that oxygen-related defects strongly trap mobile hydrogen on its diffusion pathway; however, this trapping effect becomes less effective with increasing annealing temperature. This trend strongly suggests that when wafers are subjected to

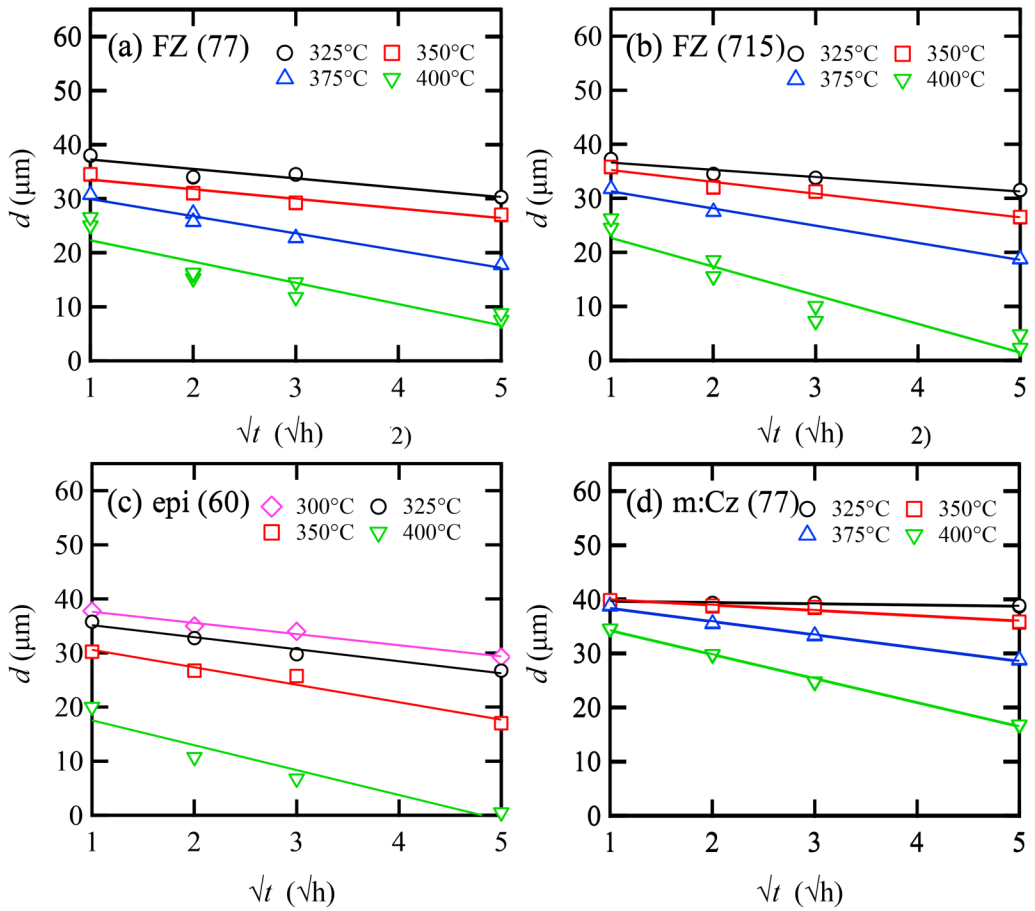

FIG. 4. Diffusion front depth of hydrogen, d, extracted from the carrier concentration profiles of the (a) FZ (77), (b) FZ (715), (c) epi (60), and (d) m:Cz (77) samples for different T and t. Diamonds, circles, squares, triangles, and inverted triangles denote annealing temperatures of 300, 325, 350, 375, and 400 °C, respectively. Solid lines are the least squares fit according to Eq. (2).

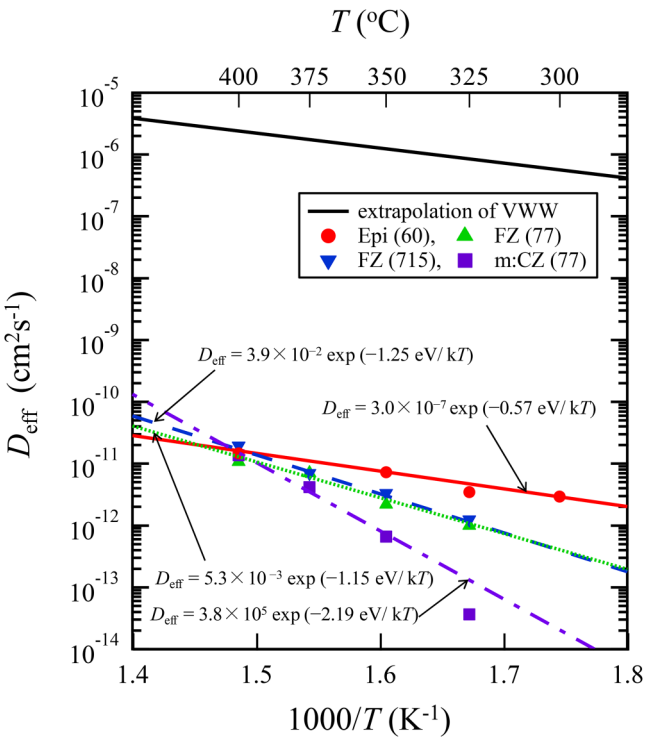

FIG. 5. Arrhenius plots for the D_{eff} of hydrogen. Circles, triangles, inverted triangles, and squares denote the data points of D_{eff} for the epi (60), FZ (77), FZ (715), and m:Cz (77) samples, respectively. Four data points almost overlap at 400 °C. Solid, dotted, dashed, and chain lines represent least squares fits of the datasets according to Eq. (1). The solid black line is the extrapolation of the early permeation data from the Van Wieringen and Warmoltz (VWW) relationship.

annealing at 400 °C, all three types of silicon materials, including m:CZ wafers, have the same diffusion coefficient in the proton irradiation doping.

In contrast, D_{eff} was less affected by carbon within the concentration range of $<5.0 \times 10^{14}$ to 1.8×10^{15} cm^{-3}. The carbon–hydrogen complex, which has a dissociation energy of 0.78 eV, is expected to be unstable at 300 °C; therefore, it is an unlikely candidate for the hydrogen trap.[38,39] Previous studies reported that the phosphorus–hydrogen complex is expected to be unstable at 300 °C[40,41] and that phosphorus has low influence on the diffusivity of hydrogen as well.

Effective diffusion coefficient was approximated according to Eq. (1) as follows: $D_{eff} = 3.0 \times 10^{-7}$ exp $(-0.57 \pm 0.15$ eV/$kT)$ cm^2/s for the epi (60), $D_{eff} = 5.3 \times 10^{-3}$ exp $(-1.15 \pm 0.1$ eV/$kT)$ cm^2/s for the FZ (77), and $D_{eff} = 3.9 \times 10^{-2}$ exp $(-1.25 \pm 0.1$ eV/$kT)$ cm^2/s for the FZ (715) (solid, dotted, and dashed lines in Fig. 5, respectively). Except at 300 °C, which deviates from Eq. (1), D_{eff} for m:Cz (77) was approximated by a line as $D_{eff} = 3.8 \times 10^{5}$ exp $(-2.19 \pm 0.15$ eV/$kT)$ cm^2/s (chain line in Fig. 5). It should be mentioned that the deduced activation energy is merely the effective value, which includes the contribution of the binding energy between hydrogen and irradiation-induced defects.

The activation energy for the diffusion of hydrogen in silicon has been investigated both experimentally and theoretically and was reported to be in the range of 0.48–1.5 eV.[18–37] The values depend on the types and concentrations of defects existing in the diffusion pathway of hydrogen. The obtained values (0.57–2.19 eV) are comparable to the activation energies reported for moderate temperatures.[12,13,34] For example, the value obtained for FZ silicon is in good agreement with the results of Refs. 12 and 13, where Laven *et al.* reported an activation energy of 1.2 eV for proton-irradiated and annealed *n*-type silicon in the range of 320–375 °C. Stein and Hahn also deduced an activation energy of 1.5 eV for trap-limited diffusion of hydrogen in the range of 350–400 °C in *n*-type silicon hydrogenated using a plasma source.[34]

In contrast, the activation energy of 0.57 ± 0.15 eV obtained in our epi wafer agrees well with the value of the VWW relationship. This result suggests that intrinsic point defects have less influence on the trapping of diffusing hydrogen. Moreover, the m:Cz sample with an oxygen concentration of up to 10^{17} cm^{-3} exhibits a large activation energy (2.19 ± 0.15 eV). These results strongly suggest that oxygen and/or oxygen-related defects play significant roles as trap centers in the trap-limited diffusion of hydrogen.

We infer that HDs serve as a reservoir for hydrogen under annealing and that oxygen-related complexes serve as a diffusion trap for hydrogen released from HDs. The dissociation energy of the oxygen-related trap centers is roughly estimated as 1.6 eV from the difference between the activation energies of hydrogen diffusivity for m:CZ and epi samples. Therefore, we should evaluate the oxygen concentration in silicon wafers to determine the width of *n*-type field-stop layers in the proton irradiation doping for power devices.

C. Dissociation of HDs

In Subsection III B, we recognized that annealing is inevitable in the creation of HDs and expansion of the *n*-type region. It was reported that annealing at excessively high temperatures (>500 °C) diminishes proton irradiation-induced HDs and that the carrier concentration is restored to its original bulk value.[12,13] This is due to the physical nature of HDs; HDs are radiation-induced point defects decorated with hydrogen, they dissociate thermally and release hydrogen at excessively high temperatures. The thermal stability of HDs seems to limit the maximum thermal budget in the implementation of the proton irradiation doping.

Here, we present the results of the dissociation of HDs to gain insight into the limitations of the annealing conditions for the doping process. The SR profiles shown in Fig. 3 clearly indicate that the maximum carrier concentration $N(t)$ monotonically decreases with increasing annealing time, t, at temperatures of >350 °C, regardless of the silicon material. In Fig. 6(a), $N(t)$ obtained at 350, 375, and 400 °C are plotted as a function of t. The decay of $N(t)$ was fitted by a line, assuming first-order kinetics of decay, which is expressed as

$$N(t) = N_o \exp(-t/\tau), \quad (3)$$

where N_o is the value of $N(t)$ at $t = 1$ h at each annealing temperature and τ is the time constant for the decay. If the decay is caused by the

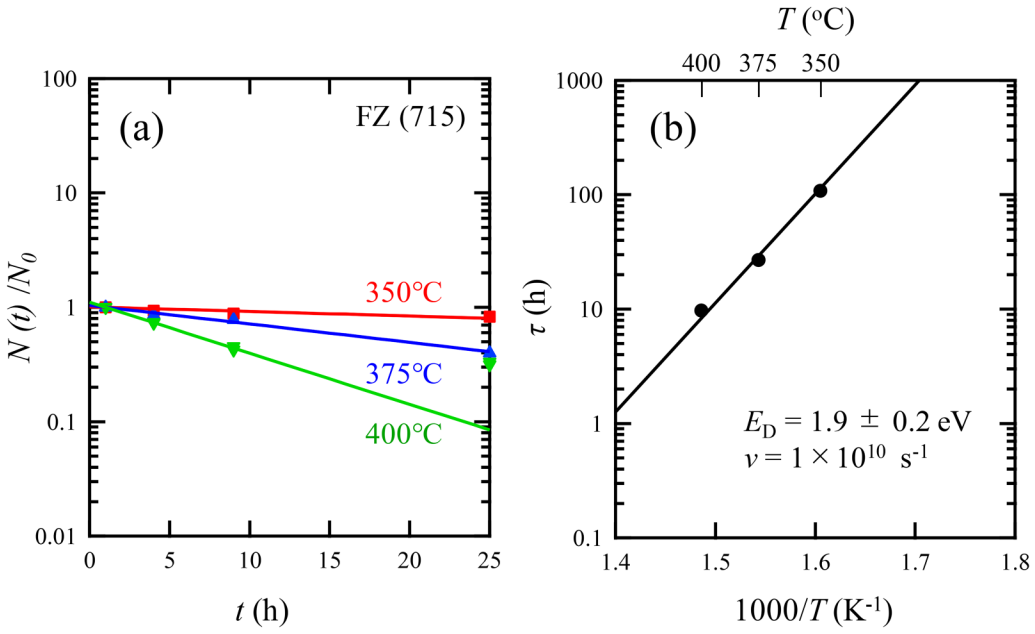

FIG. 6. (a) Decay of the normalized maximum carrier concentration $N(t)$ as a function of annealing time, t. (b) Arrhenius plot for time constant τ of dissociation of hydrogen-related donors (HDs). Maximum carrier concentration was extracted from sets of spreading resistance profiles of the FZ (715) samples. Solid colored and black lines are least squares fits of the dataset according to Eqs. (3) and (4), respectively. The green line fit (400 °C) in (a) was done only to three data points below 10 h except at 25 h.

thermally activated dissociation of HDs, τ is expressed as

$$\tau^{-1} = \nu \exp(-E_D/kT), \quad (4)$$

where ν is the attempt frequency and E_D is the dissociation energy of the HDs.

Figure 6(b) shows the Arrhenius plot of time constant τ as a function of the reciprocal temperature. Fitting analysis according to Eq. (4) determined that E_D is 1.9 ± 0.2 eV and ν is 1×10^{10} s^{-1}. The magnitude of ν suggests that the limiting process for the dissociation of HDs is due to an atomic jump process.

IV. CONCLUSIONS

N-type silicon wafers with different carbon, oxygen, and phosphorus concentrations were subjected to 2 MeV proton irradiation with a dose of 3×10^{14} cm^{-2} and subsequent annealing at various temperatures (300–400 °C) and times (1–25 h). The SR profiles show that an additional *n*-type region formed in the vicinity of the proton penetration depth, where HDs were induced; this *n*-type region expanded toward the surface with increasing annealing time at a given temperature. This expansion is attributed to the out-diffusion of implanted hydrogen through its penetrated layers. The effective diffusion coefficient extracted from the SR profiles is five to six orders of magnitude lower than the intrinsic diffusion coefficient extrapolated from the VWW relationship measured in a high temperature range and exhibit clear dependency on oxygen concentration in the range of $<5 \times 10^{15}$ to 1.8×10^{17} cm^{-3}. The effective activation energy of hydrogen diffusion was estimated to be 0.57 ± 0.15 eV for the epitaxial silicon, 1.15 ± 0.10 eV and 1.25 ± 0.10 eV for the two types of FZ wafers, and 2.19 ± 0.15 eV for the m:Cz wafer. These results indicate that oxygen-related defects serve as a diffusion trap of hydrogen released from HDs and the dissociation energy of the diffusion trap centers is approximately 1.6 eV. Therefore, the oxygen concentration is an important parameter in determining the width of the *n*-type region in the doping process, where proton irradiation and subsequent annealing are used to produce power devices. This study also reveals that the annealing process at 400 °C suppressed the dependence of hydrogen diffusivity on the oxygen concentration of silicon wafers. The dissociation energy of HDs was estimated to be 1.9 ± 0.2 eV based on the first-order kinetics of the dissociation process. This dissociation energy is considered to limit the maximum width of the *n*-type field-stop layers induced by single proton irradiation. This study provides an insight into the influence of impurities on the diffusivity of hydrogen; the results are essential to realize the cost-effective production of power devices using m:Cz wafers.

ACKNOWLEDGMENTS

The authors would like to thank J. Ito (SHI-ATEX Co., Ltd) and S. Sawada (Melco Semiconductor Engineering Corp.) for their help with the proton irradiation experiment and spread resistance measurements, respectively. The authors also thank Y. Kamiura (Professor emeritus of Okayama University) for helpful discussions and critical review of this manuscript.

DATA AVAILABILITY

The data that support the findings of this study are available within the article.

REFERENCES

[1]H. Yamamoto and T. Hashizume, Phys. Status Solidi C **8**, 662 (2011).
[2]H. J. Schulze, H. Öfner, F.-J. Niedernostheide, J. G. Laven, H. P. Felsl, S. Voss, A. Schwagmann, M. Jelinek, N. Ganagona, A. Susiti, T. Wübben, W. Schustereder, A. Breymesser, M. Stadtmüller, A. Schulz, T. Kurz, and F. Lükermann, in *Proceedings of the 28th International Symposium on Power Semiconductor Devices & ICs (ISPSD), Prague, Czech Republic* (IEEE, 2016), Vol. 355.
[3]F. Shimura, J. Appl. Phys. **59**, 3251 (1986).
[4]K. Takano, A. Kiyoi, and T. Minato, in *Proceedings of the 27th International Symposium on Power Semiconductor Devices & ICs (ISPSD), Hong Kong, China* (IEEE, 2015), Vol. 129.
[5]K. Nakamura, S. Nishizawa, and A. Furukawa, IEEE Trans. Electron Devices **67**, 2437 (2020).
[6]Y. Zohta, Y. Ohmura, and M. Kanazawa, Jpn. J. Appl. Phys. **10**, 532 (1971).
[7]K. Irmscher, H. Klose, and K. Maass, J. Phys. C Solid State Phys. **17**, 6317 (1984).
[8]J. Hartung and J. Weber, Phys. Rev. B **48**, 14161 (1993).
[9]H. Hatakeyama, M. Suezawa, V. P. Markevich, and K. Sumino, Mater. Sci. Forum **196-201**, 939 (1995).
[10]Y. Tokuda, A. Ito, and H. Ohshima, Semicond. Sci. Technol. **13**, 194 (1998).
[11]K. A. Abdullin, Y. V. Gorelkinskii, B. N. Mukashev, and A. S. Serikkanov, Physica B **340–342**, 692 (2003).
[12]J. G. Laven, H.-J. Schulze, V. Häublein, F.-J. Niedernostheide, H. Schulze, H. Ryssel, and L. Frey, Phys. Status Solidi C **8**(3), 697 (2011).
[13]J. G. Laven, R. Job, H.-J. Schulze, F.-J. Niedernostheide, W. Schustereder, and L. Frey, ECS J. Solid State Sci. Technol. **2**, P389 (2013).
[14]J. F. Ziegler, J. P, Biersack, and U. Littmark, "The stopping and range of ions in solids," in *The Stopping and Ranges of Ions in Matter* (Pergamon Press, New York, 1984), Vol. 1.
[15]E. P. Neustroev, I. A. Antonova, V. P. Popov, V. F. Stas, V. A. Skuratov, and A. Y. Didyk, Nucl. Instrum. Methods Phys. Res. B **171**, 443 (2000).
[16]P. Hazdra and V. Komarnitskyy, Nucl. Instrum. Methods Phys. Res. B **253**, 187 (2006).
[17]L. Tsetseris, S. Wang, and S. T. Pantelides, Appl. Phys. Lett. **88**, 051916 (2006).
[18]A. Van Wieringen and N. Warmoltz, Physica **22**, 849 (1956).
[19]T. Ichimiya and A. Furuichi, Int. J. Appl. Radiat. Isot. **19**, 573 (1968).
[20]S. J. Pearton, W. L. Hansen, E. E. Haller, and J. M. Kahn, J. Appl. Phys. **55**, 1221 (1984).
[21]A. Mogro-Campero, R. P. Love, and R. Schubert, J. Electrochem. Soc. **132**, 2006 (1985).
[22]M. Capizzi and A. Mittiga, Appl. Phys. Lett. **50**, 918 (1987).
[23]C. H. Seager and R. A. Anderson, Appl. Phys. Lett. **53**, 1181 (1988).
[24]C. G. Van de Walle, P. J. H. Denteneer, Y. Bar-Yam, and S. T. Pantelides, Phys. Rev. B **39**, 10791 (1989).
[25]C. P. Herrero, M. Stutzmann, A. Breitschwerdt, and P. V. Santos, Phys. Rev. B **41**, 1054 (1990).
[26]R. C. Newman, J. H. Tucker, A. R. Brown, and S. A. McQuaid, J. Appl. Phys. **70**, 3061 (1991).
[27]N. M. Johnson and C. Herring, Phys. Rev. B **43**, 14297 (1991).
[28]S. J. Pearton, J. W. Corbett, and J. T. Borenstein, Physica B **170**, 85 (1991).
[29]R. Rizk, P. de Mierry, D. Ballutaud, M. Aucouturier, and D. Mathiot, Phys. Rev. B **44**, 6141 (1991).
[30]T. Zundel and J. Weber, Phys. Rev. B **46**, 2071 (1992).
[31]B. L. Sopori, K. Jones, and X. J. Deng, Appl. Phys. Lett. **61**, 2560 (1992).
[32]P. V. Santos and W. B. Jackson, Phys. Rev. B **46**, 4595 (1992).
[33]G. Panzarini and L. Colombo, Phys. Rev. Lett. **73**, 1636 (1994).
[34]H. J. Stein and S. Hahn, J. Electrochem. Soc. **142**, 1242 (1995).
[35]A. G. Ulyashin, R. Job, I. A. Khorunzhii, and W. R. Fahrner, Physica B **308–310**, 185 (2001).
[36]C. Herring, N. M. Johnson, and C. G. Van de Walle, Phys. Rev. B **64**, 125209 (2001).
[37]Y. L. Huang, Y. Ma, R. Job, and A. G. Ulyashin, J. Appl. Phys. **96**, 7080 (2004).
[38]Y. Kamiura, M. Yoneta, and F. Hashimoto, Appl. Phys. Lett. **59**, 3165 (1991).
[39]A. L. Endrös, W. Krühler, and F. Koch, J. Appl. Phys. **72**, 2264 (1992).
[40]J. Zhu, N. M. Johnson, and C. Herring, Phys. Rev. B **41**, 12354 (1990).
[41]S. J. Pearton and J. Lopata, Appl. Phys. Lett. **59**, 2841 (1991).